

Research Paper
Dental Implants

The impact of a modified cutting flute implant design on osseointegration

R. Jimbo, N. Tovar, C. Marin, H. S. Teixeira, R. B. Anchieta, L. M. Silveira, M. N. Janal, J. A. Shibli, P. G. Coelho: *The impact of a modified cutting flute implant design on osseointegration. Int. J. Oral Maxillofac. Surg. 2014; 43: 883–888.* © 2014 International Association of Oral and Maxillofacial Surgeons. Published by Elsevier Ltd. All rights reserved.

R. Jimbo¹, N. Tovar², C. Marin³,
H. S. Teixeira², R. B. Anchieta²,
L. M. Silveira², M. N. Janal⁴,
J. A. Shibli⁵, P. G. Coelho^{2,6}

¹Department of Prosthodontics, Faculty of Odontology, Malmö University, Malmö, Sweden; ²Department of Biomaterials and Biomimetics, New York University College of Dentistry, New York, USA; ³Department of Dentistry, UNIGRANRIO, Duque de Caxias, RJ, Brazil; ⁴Department of Epidemiology, New York University College of Dentistry, New York, USA; ⁵Department of Periodontology, Dental Research Division and Oral Implantology Clinic, Guarulhos University, Guarulhos, SP, Brazil; ⁶Department of Periodontology and Implant Dentistry, New York University College of Dentistry, New York, USA

Abstract. Information concerning the effects of the implant cutting flute design on initial stability and its influence on osseointegration *in vivo* is limited. This study evaluated the early effects of implants with a specific cutting flute design placed in the sheep mandible. Forty-eight dental implants with two different macro-geometries (24 with a specific cutting flute design – Blossom group; 24 with a self-tapping design – DT group) were inserted into the mandibular bodies of six sheep; the maximum insertion torque was recorded. Samples were retrieved and processed for histomorphometric analysis after 3 and 6 weeks. The mean insertion torque was lower for Blossom implants ($P < 0.001$). No differences in histomorphometric results were observed between the groups. At 3 weeks, $P = 0.58$ for bone-to-implant contact (BIC) and $P = 0.52$ for bone area fraction occupied (BAFO); at 6 weeks, $P = 0.55$ for BIC and $P = 0.45$ for BAFO. While no histomorphometric differences were observed, ground sections showed different healing patterns between the implants, with better peri-implant bone organization around those with the specific cutting flute design (Blossom group). Implants with the modified cutting flute design had a significantly reduced insertion torque compared to the DT implants with a traditional cutting thread, and resulted in a different healing pattern.

Key words: implants; cutting flute design; macro-geometry; thread design; insertion torque; histomorphometry; primary stability; secondary stability; osseointegration.

Accepted for publication 30 January 2014
Available online 28 February 2014

The initial stability of an implant is essential for achieving osseointegration. This is affected by the mechanical stability achieved due to different surgical procedures, such as altering the drilling technique,^{1–3} and also by the friction between the implant and the bone.⁴ With high initial stability it is possible for the implant to interact with growth factors and proteins, which induces osteogenic cell

migration to the implant surface.⁵ If, in the early stages of healing, the implant is not in an immobile state, the biological pendulum will shift towards soft tissue induction around the implant surface, which may result in fibrous encapsulation.⁶ The so-called micromotion of the implant has been studied extensively and it is generally agreed that this phenomenon, when over 150 μm , leads to tissue

damage and triggers negative biological bone healing responses.^{7,8}

It has also been stated that a high initial torque is one of the requirements for obtaining primary initial stability. A study conducted on fresh bovine bone showed that higher insertion torque on a specific implant reduced the amount of micromotion, suggesting that there is an inverse relationship between the two factors.⁹

Furthermore, it was demonstrated in some clinical studies that an implant with a modified macro-geometry generated higher insertion torque and was more suitable for immediate provisionalization when compared to the conventional straight wall design implants.^{10,11} In contrast, a previous long-term clinical study reported that a low rotational stability at the time of implant insertion is not an indication for delayed loading, and suggested that there may be a misconception with regard to what is actually correlated with primary stability or a low level of micromotion.¹² In that study, implants with a low insertion torque of 25 Ncm were immediately loaded and clinical follow-up was conducted. The results showed a minimum amount of marginal peri-implant bone loss, with high survival rates, suggesting that implant osseointegration may not have a linear relationship with insertion torque values.

In addition, implant insertion torque and the relationship with micromotion may also depend on the cutting feature design. In a previous bench study, the insertion torque and micromotion of implants with the same macro-geometry, with or without cutting features, were recorded.¹³ It was shown that implants with a specific cutting feature placed in polyurethane foam blocks significantly decreased not only the insertion torque, but also the micromotion. Changing the implant architecture to include a more efficient a cutting flute decreases the insertion torque, since it reduces the friction forces.^{14,15} Compression and an increased shear force may destroy the supporting bone structure, which consequently lowers the initial stability.^{5,16}

Many of the studies investigating the effect of implant geometry on rotational forces have been conducted on Sawbone or similar material.^{15,17,18} However, a limitation of these *in vitro* studies is that it is uncertain whether the material used is actually simulating the biomechanical properties of cortical and cancellous bone.¹⁵ Also, information regarding the biological effects of the cutting flute design on initial stability *in vivo* and its influence on osseointegration (secondary stability) is limited.

Hence, in order to evaluate purely the effect of the cutting flute, implants with the same macro-geometry with or without a modified cutting flute were utilized in the present study. The objective of this study was to evaluate the early biological effects of implants with a specific cutting flute design placed in the sheep mandibular model. Since this model resembles the human mandible, the outcomes may be related to the actual situation in the oral

cavity. The biological responses were evaluated histologically and histomorphometrically.

Materials and methods

This animal study was performed in accordance with the ARRIVE guidelines, and the relevancy of the animal selection and use of animals were considered carefully.

Implant macro-geometry

The present study evaluated two different implant macro-geometries: Blossom ($n = 24$ implants) and DT classic self tapping design. ($n = 24$ implants) designs, both with the Ossean surface treatment (Intra-Lock International Inc., Boca Raton, FL, USA) (Fig. 1).

Animals and surgery

Six sheep (approximately 2 years of age) were used for the study. Bioethics committee approval was obtained.

The central region of the mandibular body on the lateral aspect was chosen for the procedure. All procedures were performed under general anaesthesia. Pre-anaesthesia consisted of intravenous (i.v.) thiopental (15 mg/kg), followed by orotracheal intubation. Inhalational general anaesthesia was maintained with isoflurane (2.5%), intramuscular (i.m.) ketamine (0.2 mg/kg), and meloxicam (0.5 mg/kg i.m.). After shaving and exposing the skin,

an antiseptic solution containing iodine was applied to the surgical site, as well as the surrounding area. A 5-cm incision was made parallel to the inferior border of the mandible. The platysma was dissected and cut in order to reach the periosteum, which was subsequently incised and reflected with a periosteal elevator. Finally, the mandibular body was exposed using manual retractors. The four-implant sites were prepared by drilling at 900 rpm under abundant saline irrigation, in accordance with the manufacturer's recommendations. The implants were placed in a line at 1 cm intervals, approximately 2 cm above the basal border of the mandibular body. Each animal received two Blossom implants and two DT implants in an interpolated fashion. For instance, a Blossom, a DT, a Blossom, and a DT were placed from distal to proximal in the first animal, and a DT, a Blossom, a DT, and a Blossom were placed from distal to proximal in the second animal. This approach resulted in balanced surgical procedures that allowed the comparison of the same number of implant surfaces by time *in vivo*, limb, surgical site (1 through 4), and animal. The implants were inserted in the drilled sites, and the maximum insertion torque was recorded with a portable digital torque metre (Tohnichi, Tokyo, Japan), with a 200 Ncm load cell for each implant placed. In the first surgical procedure, 24 implants were placed in the left mandible; a further 24 implants were placed in the contralateral side at second surgery 3 weeks later. Thus the implants

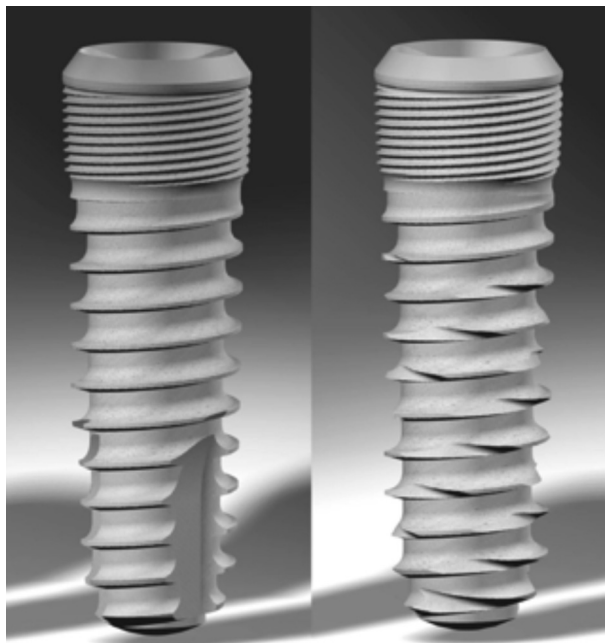


Fig. 1. The two different implant designs used in the current study. Left: Self Tapping, Right Blossom.

remained in place *in vivo* for 6 weeks on the left side and 3 weeks on the right.

The surgical sites were sutured layer by layer (internal layers: 3–0 vicryl; skin: 3–0 nylon). Postoperatively, all animals were given antibiotics (benzylpenicillin 15 mg/kg and dihydrostreptomycin 20 mg/kg, *i.m.*) for 5 days, analgesics on the skin (fentanyl patch, 3 µg/h/kg, effect over 3 days), and an anti-inflammatory for 2 days (meloxicam 0.5 mg/kg, *i.m.*). No signs of infection or other complications were observed during the postoperative period. Euthanasia by anaesthetic overdose was performed after 6 weeks, and the mandibular body was retrieved. After careful removal of the surrounding soft tissue, the surgical site was exposed and implant stability was checked. Thereafter, all samples were subjected to histological processing.

Histological processing and histomorphometric analysis

The bones containing the implants were reduced to blocks and immersed in 10% buffered formalin solution for 24 h. The blocks were then washed in running water for 24 h, and steadily dehydrated in a series of alcohol solutions ranging from 70% to 100% ethanol. Following dehydration, the samples were embedded in a methacrylate-based resin (Technovit 9100; Heraeus Kulzer GmbH, Wehrheim, Germany) following the manufacturer's instructions. The blocks were then cut into slices (~300 µm thickness) aiming at the centre of the implant along its long axis with a precision diamond saw (IsoMet 2000; Buehler Ltd., Lake Bluff, IL, USA). The slices were glued to acrylic plates with an acrylate-based cement and left for 24 h to set prior to grinding and polishing. The sections were then reduced to a final thickness of ~30 µm by means of a series of silicon carbide abrasive papers (SiC 400, 600, 800, 1200, and 2400; Buehler Ltd., Lake Bluff, IL, USA) in a grinding/polishing machine (MetaServ 3000, Buehler Ltd., Lake Bluff, USA) under water irrigation.¹⁹ The sections were then stained with toluidine blue and submitted to optical microscopy at 50–200× magnification (Leica DM2500M; Leica Microsystems GmbH, Wetzlar, Germany) for histomorphological evaluation.

The bone-to-implant contact (BIC) was determined at 50–200× magnification (Leica DM2500M) using computer software (Leica Application Suite; Leica Microsystems GmbH, Wetzlar, Germany). The regions of bone-to-implant contact along the implant perimeter were

subtracted from the total implant perimeter, and calculations were performed to determine the BIC. The bone area fraction occupied (BAFO) between threads in trabecular bone regions was determined at 100× magnification (Leica DM2500M) by means of computer software (Leica Application Suite). The areas occupied by bone were subtracted from the total area between threads, and calculations were performed to determine the BAFO (reported in percentage values of bone area fraction occupied).²⁰

In order to test the null hypothesis that no differences in insertion torque and biological outcomes (BIC and BAFO) exist between the two different implant designs, statistical analyses were performed using IBM SPSS v. 20 software (IBM Corp., Armonk, NY, USA). Preliminary statistical analyses showed no effect of implant site (*i.e.*, there were no consistent effects of different positions along the mandible) on any measurement. Therefore, site was collapsed in the further analysis. Box plots were used to show the range and distribution of each dependent measure as a function of time and implant design. There were six animals, and each received both implant designs twice at two different times *in vivo*. Thus, the primary statistical evaluation of the effects of time and implant design on torque, BIC, and BAFO was done with two-way mixed model analysis of variance (ANOVA), with one grouping (time *in vivo*) and a repeated factor (implant design), each at two levels while estimating a random intercept. Post hoc comparisons were done with a *t*-test based on the pooled standard error. Statistical significance was set at 5%, based on the result of either test ($\alpha \leq 0.05$).

Results

A total of 48 dental implants of two different macro-geometries were inserted into the mandibular bodies of six sheep. The surgical procedures and follow-up presented no complications regarding procedural conditions or other immediate clinical concerns. No postoperative complication was detected and no implant was excluded from the study.

The insertion torque recorded for each group is presented in Fig. 2. The torque was significantly lower for the Blossom implants relative to the DT implants ($P < 0.001$).

Histomorphometric evaluation (Fig. 3) showed a remarkably similar pattern for both BIC and BAFO values. A significant increase was detected for both parameters from week 3 to week 6 ($P < 0.01$ for both groups), and no significant differences were noted between the implant groups at 3 or 6 weeks *in vivo* ($P > 0.45$).

Qualitative evaluation of the biological response showed close contact between cortical and trabecular bone for both groups at both implantation times, including regions that were in close proximity or substantially distant from the osteotomy walls.

Despite the similar BIC and BAFO values, different healing patterns were observed for the two different implant designs (Figs. 4–7). At 3 weeks, the bone around the DT implant presented two very distinct regions (Fig. 4). The first, the empty space that was present immediately after placement due to the geometric interplay between implant bulk and instrumentation (healing chambers) presented substantial bone formation (Fig. 4a). However, regions where primary engagement

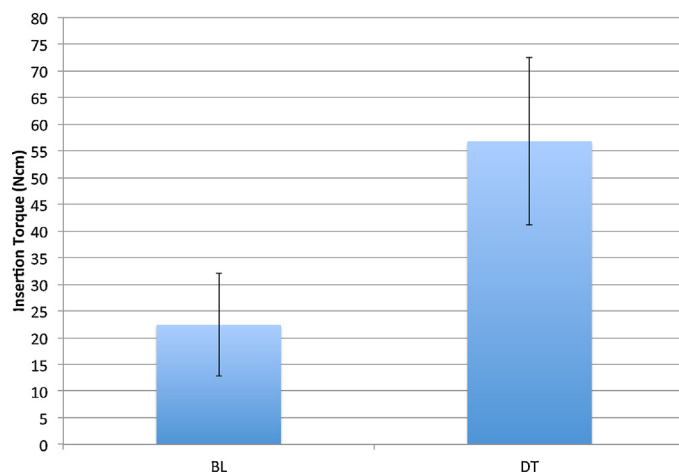


Fig. 2. Insertion torque. A significant difference in the insertion torque was observed between the study groups ($P < 0.001$); BL, blossom implants; DT, DT implants. Data are presented as the mean \pm SD.

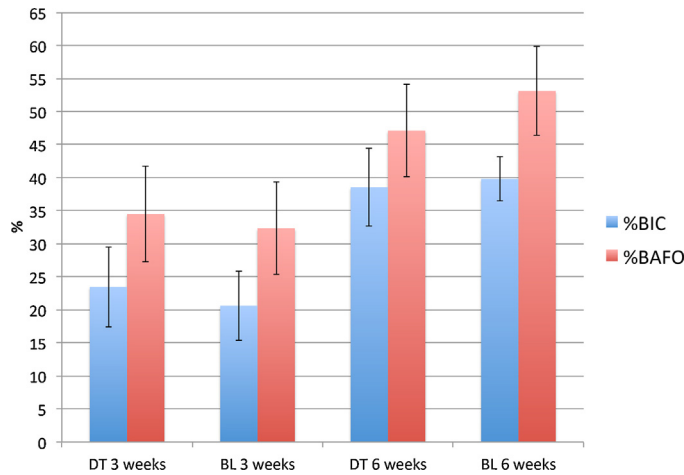


Fig. 3. BIC (bone-to-implant contact) and BAFO (bone area fraction occupied) values at 3 and 6 weeks. A similar pattern for both BIC and BAFO values was observed, in which a significant increase was found for both parameters from 3 to 6 weeks ($P < 0.01$ for both), and no significant differences were detected between the groups at 3 or at 6 weeks *in vivo*. At 3 weeks $P = 0.58$ for BIC and $P = 0.52$ for BAFO. At 6 weeks, $P = 0.55$ for BIC and $P = 0.45$ for BAFO. Data are presented as the mean \pm SD.

and bone compression between implant and bone occurred immediately after implantation (the thread tips) presented several areas of bone resorption by multinucleated cells (Fig. 4b). At 6 weeks, higher degrees of contact were observed between implant and bone, primarily in the healing chamber regions (Fig. 5). However, despite higher amounts of bone filling the regions between implant threads, several areas of bone resorption by multinucleated cells were also consistently observed in the bone regions adjacent to the thread tips where a high concentration of stress occurs during placement.

At 3 weeks *in vivo*, in the same manner as described for the DT implant design, histology of the Blossom implants showed contact between implant and bone being reestablished in an intramembranous-like fashion due to formation of the healing

chamber between the implant and old bone immediately after placement (Fig. 6a). Higher magnification of the bone region between threads showed bone chips originating from the cutting threads to be present along the length of the implant, acting as nucleating sites for new bone formation (Fig. 6b). Very few resorption/remodelling sites were observed in the thread tip regions of the Blossom implants, unlike the DT implants (Fig. 6a). At 6 weeks, higher amounts of bone were observed occupying the healing chamber regions (Fig. 7) around the Blossom implants. Unlike the bone present at 6 weeks around the DT implants, bone in the region of the healing chambers next to the Blossom implants presented primary osteonic structures along with bone chips embedded in newly formed bone.

Discussion

This study investigated the biological influence of an implant with a modified cutting flute design in a sheep mandibular model. The insertion torque values were significantly lower for the Blossom implants than for the DT implants. However the histomorphometric analysis at both 3 and 6 weeks were similar ($P > 0.05$) for both the DT and Blossom implants, despite remarkable differences in healing patterns.

The cutting flute design of the Blossom implant is unique, since there is a cutting feature on every thread. This is different to the traditional cutting flute designs of the so-called 'self-tapping' implant systems, in which there is a cutting feature only on the apical portion of the implant. This type of cutting edge normally guides the implant into the osteotomy site, which is prepared to be slightly smaller than the actual diameter of the implant thus decreasing wobbling.^{15,21,22}

In detail, in the use of the traditional design implant, the insertion torque undergoes several changes during implant insertion.¹⁶ First, the cutting feature in the apical region increases the torque as it cuts a thread in the cortical region. In the next phase, the insertion torque increases further during the gradual transition in implant diameter, which is generated by friction and static strain. Finally, when the cut thread in the bone matches the implant thread, and no more expansion is required, the insertion torque values even out. In contrast, the Blossom implant design is of interest because the cutting phase is continuous and could release the strain during expansion. This is thought to be the major reason for the reduced insertion torque observed in the current *in vivo* study, and in a previous *in vitro* study.¹³

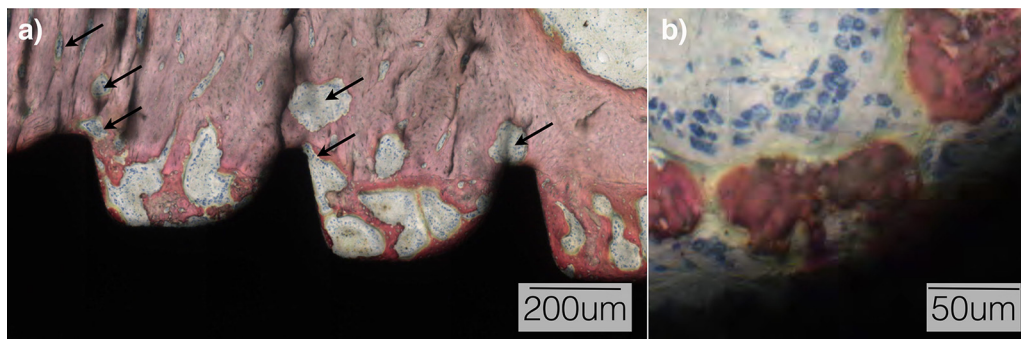


Fig. 4. DT implant optical micrographs at 3 weeks *in vivo*. (a) The interface where contact between the implant and the bone is being reestablished in an intramembranous-like fashion due to the formation of a healing chamber between the implant and old bone immediately after placement. Several areas of bone resorption by multinucleated cells were also consistently observed in bone regions adjacent to the thread tips (arrows), where a high concentration of stress occurs during placement. (b) Higher magnification of a thread tip bone region showing multinucleated cell-based bone resorption.



Fig. 5. DT implant optical micrograph at 6 weeks *in vivo* showing the interface where contact between the implant and bone has been reestablished in an intramembranous-like fashion due to the formation of a healing chamber between the implant and old bone immediately after placement. Despite higher amounts of bone filling in the regions between implant threads, several areas of bone resorption by multinucleated cells were also consistently observed in bone regions adjacent to the thread tips, where a high concentration of stress occurs during placement.

It has been stated that a press-fit design increases the resistance to micromotion compared to a non-press-fit situation.²³ Although the press-fit implant provides close contact between the implant and the bone, and in general provides high insertion torque values, it has been suggested that the bone initially in contact with the implant is gradually resorbed and is altered by newly formed bone.²⁴ This is probably due to the excessive strain or compression on the press-fit regions that exceeds the physiological limit, triggering bone resorption.²⁵

Regardless of the compression forces, it is also a fact that the trauma of surgery results in necrotic bone around the implant.²⁶ It can be said that the necrotic bone supporting the implant is involved in the initial mechanical stability,²⁷ and strains below the physiological limit may maintain the bone with adequate stimulation forces that contribute to

eventual bone apposition.⁶ Thus, it appears logical to suggest that insertion torque and primary stability may be two totally different factors, which is in agreement with the literature.¹²

The observation of multinucleated giant cells in the vicinity of the DT implants suggests that some bone remodelling activity was ongoing, probably due to the high levels of strain at the thread tips engaging the bone immediately after implantation, resulting in high insertion torque levels. However at the same time, active new bone formation was visible on the histological micrographs in the areas where implant and bone were loosely fit in the healing chamber regions, and the corresponding histomorphometric outcomes presented high BIC and BAFO values. This suggests that the strain generated by the DT implant thread tips was slightly higher than the physiological limit, resulting in

a negative biological reaction (bone remodelling) in those regions. What is of great importance is that the Blossom implants with the cutting flutes on each thread presented lower insertion torque values but comparable osseointegration to the control implants, with no visible signs of multinucleated giant cells and thereby resorption in the vicinity of the implant. This is an indication that the implants were inserted with adequate force, resulting in almost absent bone remodelling sites over time, which will consequently result in lower levels of micromotion essential for new bone formation. Moreover, the bone debris particles seen in the magnified histograms acted as a core for new bone formation, and this is another unique finding with regard to the implants with cutting flutes in the current study. This finding is in accordance with the results of the study by Bosshardt et al., who reported that these particles enhanced new bone formation around their hydrophilic implants.²⁸ Since higher strain is destructive to the surrounding bone and may create micro-fractures and transient large empty spaces during the early stages of osseointegration due to bone resorption, implants that can be inserted with lower insertion torque may lead to enhanced osseointegration.

In conclusion, the Blossom implants with a modified cutting flute design significantly reduced the insertion torque compared to the DT implants with a traditional cutting thread, and resulted in a different healing pattern that may be beneficial in reducing micromotion levels during osseointegration. Although the insertion torque was significantly reduced for the cutting flute design, the biological outcomes were comparable. Thus, the null hypothesis was rejected.

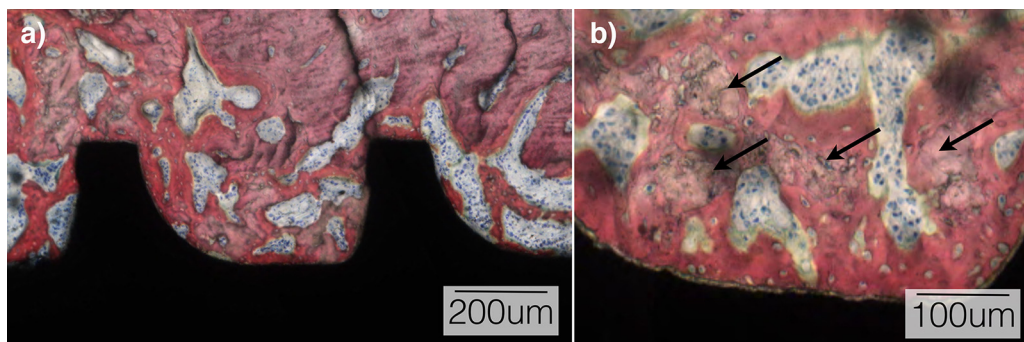


Fig. 6. Blossom implant optical micrographs at 3 weeks *in vivo*. (a) The interface where contact between the implant and bone is being reestablished in an intramembranous-like fashion due to the formation of a healing chamber between the implant and old bone immediately after placement. (b) Higher magnification of the bone region between threads shows that bone chips (arrows) originating from the cutting threads act as nucleating sites for new bone formation.

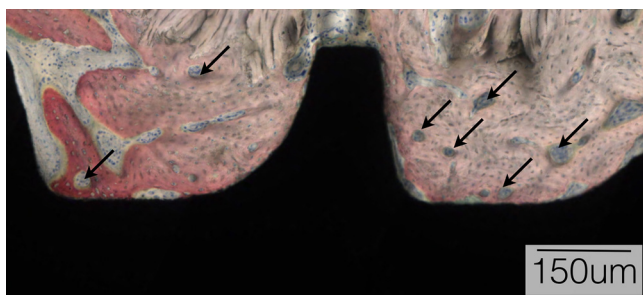


Fig. 7. Blossom implant optical micrographs at 6 weeks *in vivo*. At 6 weeks, bone around the Blossom implant design presented primary osteonic structures (arrows) in the healing chamber regions, along with bone chips embedded in newly formed bone.

Funding

This study was funded by Intra-Lock International (Boca Raton, FL, USA).

Competing interests

The authors declare no conflicts of interest.

Ethical approval

The bioethics committee of l'Ecole Nationale Vétérinaire Maisons-Alfort, Paris, France, approved this study.

References

1. Jimbo R, Giro G, Marin C, Granato R, Suzuki M, Tovar N, et al. Simplified drilling technique does not decrease dental implant osseointegration: a preliminary report. *J Periodontol* 2013;**84**:1599–605.
2. Campos FE, Gomes JB, Marin C, Teixeira HS, Suzuki M, Witek L, et al. Effect of drilling dimension on implant placement torque and early osseointegration stages: an experimental study in dogs. *J Oral Maxillofac Surg* 2012;**70**:e43–e.
3. Giro G, Marin C, Granato R, Bonfante EA, Suzuki M, Janal MN, et al. Effect of drilling technique on the early integration of plateau root form endosteal implants: an experimental study in dogs. *J Oral Maxillofac Surg* 2011;**69**:2158.
4. Hudieb MI, Wakabayashi N, Kasugai S. Magnitude and direction of mechanical stress at the osseointegrated interface of the microthread implant. *J Periodontol* 2011;**82**:1061.
5. Halldin A, Jimbo R, Johansson CB, Wennerberg A, Jacobsson M, Albrektsson T, et al. Implant stability and bone remodeling after 3 and 13 days of implantation with an initial static strain. *Clin Implant Dent Relat Res* 2012;(October). [Epub ahead of print].
6. Chowdhary R, Jimbo R, Thomsen C, Carlsson L, Wennerberg A. Biomechanical evaluation of macro and micro designed screw-type implants: an insertion torque and removal torque study in rabbits. *Clin Oral Implants Res* 2013;**24**:342–6. <http://dx.doi.org/10.1111/i.1600-0501.2011.02336.x>.
7. Gao SS, Zhang YR, Zhu ZL, Yu HY. Micromotions and combined damages at the dental implant/bone interface. *Int J Oral Sci* 2012;**4**:182.
8. Winter W, Klein D, Karl M. Effect of model parameters on finite element analysis of micromotions in implant dentistry. *J Oral Implantol* 2013;**39**:23–9. <http://dx.doi.org/10.1563/AAID-JOI-D-11-00221>.
9. Trisi P, Perfetti G, Baldoni E, Berardi D, Colagiovanni M, Scogna G. Implant micromotion is related to peak insertion torque and bone density. *Clin Oral Implants Res* 2009;**20**:467.
10. Irinakis T, Wiebe C. Initial torque stability of a new bone condensing dental implant. A cohort study of 140 consecutively placed implants. *J Oral Implantol* 2009;**35**:277.
11. Irinakis T, Wiebe C. Clinical evaluation of the NobelActive implant system: a case series of 107 consecutively placed implants and a review of the implant features. *J Oral Implantol* 2009;**35**:283.
12. Norton MR. The influence of insertion torque on the survival of immediately placed and restored single-tooth implants. *Int J Oral Maxillofac Implants* 2011;**26**:1333.
13. Freitas Jr AC, Bonfante EA, Giro G, Janal MN, Coelho PG. The effect of implant design on insertion torque and immediate micromotion. *Clin Oral Implants Res* 2012;**23**:113.
14. Bickley MB, Hanel DP. Self-tapping versus standard tapped titanium screw fixation in the upper extremity. *J Hand Surg* 1998;**23**:308.
15. Wu SW, Lee CC, Fu PY, Lin SC. The effects of flute shape and thread profile on the insertion torque and primary stability of dental implants. *Med Eng Phys* 2012;**34**:797.
16. Halldin A, Jimbo R, Johansson CB, Wennerberg A, Jacobsson M, Albrektsson T, et al. The effect of static bone strain on implant stability and bone remodeling. *Bone* 2011;**49**:783.
17. Elias CN, Rocha FA, Nascimento AL, Coelho PG. Influence of implant shape, surface morphology, surgical technique and bone quality on the primary stability of dental implants. *J Mech Behav Biomed Mater* 2012;**16**:169.
18. Ahn SJ, Leesungbok R, Lee SW, Heo YK, Kang KL. Differences in implant stability associated with various methods of preparation of the implant bed: an *in vitro* study. *J Prosthet Dent* 2012;**107**:366.
19. Donath K, Breuner G. A method for the study of undecalcified bones and teeth with attached soft tissues. The Sage–Schliff (sawing and grinding) technique. *J Oral Pathol* 1982;**11**:318.
20. Leonard G, Coelho P, Polyzois I, Stassen L, Claffey N. A study of the bone healing kinetics of plateau versus screw root design titanium dental implants. *Clin Oral Implants Res* 2009;**20**:232.
21. Holmgren EP, Seckinger RJ, Kilgren LM, Mante F. Evaluating parameters of osseointegrated dental implants using finite element analysis—a two-dimensional comparative study examining the effects of implant diameter, implant shape, and load direction. *J Oral Implantol* 1998;**24**:80.
22. Friberg B, Jisander S, Widmark G, Lundgren A, Ivanoff CJ, Sennerby L, et al. One-year prospective three-center study comparing the outcome of a “soft bone implant” (prototype Mk IV) and the standard Branemark implant. *Clin Implant Dent Relat Res* 2003;**5**:71.
23. Brunski JB. Biomaterials and biomechanics in dental implant design. *Int J Oral Maxillofac Implants* 1988;**3**:85.
24. Berglundh T, Abrahamsson I, Lang NP, Lindhe J. De novo alveolar bone formation adjacent to endosseous implants. A model study in the dog. *Clin Oral Implants Res* 2003;**14**:251.
25. Bashutski JD, D’Silva NJ, Wang HL. Implant compression necrosis: current understanding and case report. *J Periodontol* 2009;**80**:700.
26. Eriksson RA, Albrektsson T, Magnusson B. Assessment of bone viability after heat trauma. A histological, histochemical and vital microscopic study in the rabbit. *Scand J Plast Reconstr Surg* 1984;**18**:261.
27. McKibbin B. The biology of fracture healing in long bones. *J Bone Joint Surg Br* 1978;**60-B**:150.
28. Bosshardt DD, Salvi GE, Huynh-Ba G, Ivanovski S, Donos N, Lang NP. The role of bone debris in early healing adjacent to hydrophilic and hydrophobic implant surfaces in man. *Clin Oral Implants Res* 2011;**22**:357.

Address:

Ryo Jimbo

Department of Prosthodontics

Faculty of Odontology

Malmö University

205 06 Malmö

Sweden

Tel: +46 40 665 8503; Fax: +46 40 665 8679

E-mail: ryo.jimbo@mah.se